

Spectral Trends of Solar Bursts at Sub-THz Frequencies

L.O.T. Fernandes¹ · P. Kaufmann^{1,2} · E. Correia^{1,3} ·
C.G. Giménez de Castro¹ · A.S. Kudaka¹ · A. Marun⁴ ·
P. Pereyra⁵ · J.-P. Raulin¹ · A.B.M. Valio¹

Received: 11 February 2016 / Accepted: 19 December 2016 / Published online: 5 January 2017
© Springer Science+Business Media Dordrecht 2017

Abstract Previous sub-THz studies were derived from single-event observations. We here analyze for the first time spectral trends for a larger collection of sub-THz bursts. The collection consists of a set of 16 moderate to small impulsive solar radio bursts observed at 0.2 and 0.4 THz by the *Solar Submillimeter-wave Telescope* (SST) in 2012–2014 at El Leoncito, in the Argentinean Andes. The peak burst spectra included data from new solar patrol radio telescopes (45 and 90 GHz), and were completed with microwave data obtained by the *Radio Solar Telescope Network*, when available. We critically evaluate errors and uncertainties in sub-THz flux estimates caused by calibration techniques and the corrections for atmospheric transmission, and introduce a new method to obtain a uniform flux scale criterion for all events. The sub-THz bursts were searched during reported GOES soft X-ray events of class C or larger, for periods common to SST observations. Seven out of 16 events exhibit spectral maxima in the range 5–40 GHz with fluxes decaying at sub-THz frequencies (three of them associated to GOES class X, and four to class M). Nine out of 16 events exhibited the sub-THz spectral component. In five of these events, the sub-THz emission fluxes increased with a separate frequency from that of the microwave spectral component (two classified as X and three as M), and four events have only been detected at sub-THz frequencies (three classified as M and one as C). The results suggest that the THz component might be present throughout, with the minimum turnover frequency increasing as a function of the energy of the emitting electrons. The peculiar nature of many sub-THz burst events requires further investigations of bursts that are examined from SST observations alone to better understand these phenomena.

✉ P. Kaufmann
pierrekau@gmail.com

¹ Centro de Rádio Astronomia e Astrofísica Mackenzie, Escola de Engenharia, Universidade Presbiteriana Mackenzie, São Paulo, SP, Brazil

² Centro de Componentes Semicondutores, Universidade Estadual de Campinas, Campinas, SP, Brazil

³ Instituto Nacional de Pesquisa Espacial (INPE), São José dos Campos, SP, Brazil

⁴ Instituto de Ciencias Astronómicas, de la Tierra y del Espacio (CONICET), San Juan, Argentina

⁵ Complejo Astronómico El Leoncito (CONICET), San Juan, Argentina

Keywords Solar flares · Sub-THz bursts · Sub-THz atmospheric transmission · Radio-bursts spectra

1. Introduction

The extension of solar observations into the sub-THz frequency range can help us to better understand the emission mechanisms involved in the flaring process. A new spectral component has been discovered whose sub-THz fluxes increase with frequency at the same time, but separate from the well-known microwave component, bringing new challenges for the interpretation (Kaufmann *et al.*, 2004; Silva *et al.*, 2007; Fleishman and Kontar, 2010; Krücker *et al.*, 2013). Early solar burst observations at frequencies of up to 100 GHz did indicate spectral trends with fluxes increasing with frequency, some exhibiting spectral structures (Shimabukuro, 1970; Croom, 1971; Akabane *et al.*, 1973; Zirin and Tanaka, 1973; Roy, 1979; Kaufmann *et al.*, 1985; White *et al.*, 1992). More recently, impulsive events were also observed at 30 THz, with fluxes several times higher than the flux of the microwave component (Kaufmann *et al.*, 2013, 2015a). However, nearly all studies of sub-THz frequencies carried so far were based on single-event observations in different observational circumstances. In the present study we analyze comparative spectral trends for a large set of events observed at 0.2 and 0.4 THz by the *Solar Submillimeter-wave Telescope* (SST) (Kaufmann *et al.*, 2001, 2008), complemented by observations at 45 and 90 GHz by solar patrol radio telescopes (POEMAS) (Valio *et al.*, 2013) and at microwaves by the *Radio Solar Telescope Network* (RSTN; Guidice, 1979). Errors in flux determination at sub-THz frequencies are critically reviewed. A convenient method to calibrate the sub-THz data has been adopted to obtain an accurate single and uniform flux scale for all analyzed bursts.

2. Sub-THz Errors in Flux

The accuracy of solar observations at sub-THz is affected by several errors and uncertainties in flux determination that become particularly critical for weak bursts or small variations in large bursts. They include inaccuracies in atmosphere transmission, corrections in noise temperature calibration, antenna beams gain determination; fluctuations caused by atmospheric propagation, and independent uncertainties in source position when using multiple overlapping beam techniques for flux estimates. We recall that all burst flux estimates assume that the burst angular sizes are smaller than the angular sizes of the beams, and that they can therefore be estimated by knowing the antenna aperture efficiency for each beam.

Transmission “window” bands at sub-THz frequencies become available at high-altitude sites (Turner *et al.*, 2012; Tremblin *et al.*, 2012). The corrections for sub-THz observations for atmospheric transmission are the main source of error, especially for higher values of the atmospheric attenuation. The atmospheric transmission correction methods have been reviewed and applied to the SST at El Leoncito by Melo *et al.* (2005).

One simpler indirect inference of attenuation is derived from the “sky” temperature variation with elevation angle (the so-called “tipping” method). It is only reliable for low attenuation values. The attenuation can be directly determined from solar signal extinction measurements taken at different elevation angles, taken at days with extremely low atmospheric attenuation (Melo *et al.*, 2005). The method allows determining the product of the

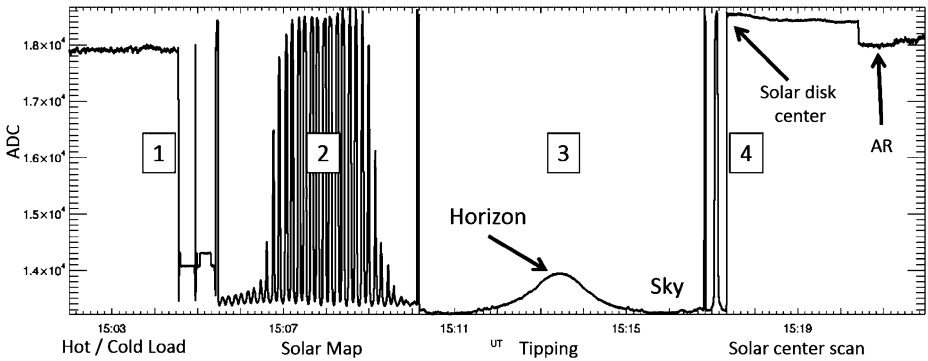


Figure 1 SST observation shown for one 0.2 THz channel during calibrations: 1) internal temperature calibration, 2) solar map scans, 3) sky temperature tipping the antenna from zenith/horizon/zenith, 4) tracking of solar center followed by active-region source tracking.

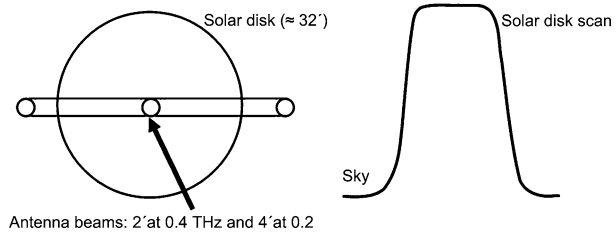
antenna beam coupling coefficient to the adopted solar brightness temperature. Although neither of these factors is precisely known, the product is well determined, allowing a direct estimate of attenuation over a much wider range of values than the tipping method (Melo *et al.*, 2005).

Figure 1 shows a sample of the actual SST observation during calibration steps, illustrating one of the six beams. SST has six independent radiometric back-ends, four at 0.2 THz with a half power beam width (HPBW) of 4 arcminutes and two at 0.4 THz, with HPBW of 2 arcminutes (see for example Giménez de Castro *et al.*, 1999; Kaufmann *et al.*, 2001, 2008). Three of the 0.2 THz beams are partially overlapped at the 3 dB levels, and the fourth is placed 8 arcminutes apart. One 0.4 THz beam is located at the center of the cluster of the three 0.2 THz beams that partially overlap, and another at a direction that is coincident with the fourth 0.2 THz beam; this is also displaced from the cluster by 8 arcminutes.

Further measurement uncertainties need to be added because of the planet brightness temperature approximations. The planet brightness temperatures and corresponding fluxes are the standard references for antenna effective aperture (and gain) calibrations. The applicable beam angular sizes are larger than the planet angular sizes. Furthermore, the antenna efficiencies at 0.2 and 0.4 THz, determined from Jupiter and Venus observations (Kaufmann *et al.*, 2001, 2008), may change with time; this is not regularly monitored. Another uncertainty arises from the internal noise temperature references, which do change with time and need to be recalibrated; this is not done on regular basis either.

A separate uncertainty in flux calculations is independent of atmospheric transmission, temperature scale, or aperture efficiencies (or gain) corrections. It is caused by the multiple-beam technique algorithm that is used to determine the centroid position of the burst source emission with respect to the partially overlapped beams of the SST. Once the position is determined, the burst flux can be estimated, assuming the burst angular size is smaller than the HPBW. The method has been fully described elsewhere (Georges *et al.*, 1989; Giménez de Castro *et al.*, 1999). The burst angular position with respect to the multiple overlapping 0.2 THz beams is obtained with an accuracy that is set by the tracking conditions, which is on the order of 1 arcmin (Kaufmann *et al.*, 2008). The corresponding impact of the multiple-beam algorithm on the flux calculation strongly depends on the several beam signal levels compared to signal baseline fluctuations. The net uncertainty may

Figure 2 Schematic diagram showing a solar disk scan by one of the SST beams, providing the derivation of the flux scale for that beam (see text).



be estimated to be smaller than about $\pm 25\%$. However, it should be emphasized that actual fluctuations in the observed signal baseline are generally dominated by atmospheric propagation variations. They become more pronounced when a) the atmospheric transmission is poor, b) for observations carried out with the Sun at low elevation angles, c) when the SST beams point to flaring sites near the solar limb when some beams are partially filled by the disk emission, and therefore respond more strongly to tracking irregularities.

3. A Simple Method for Uniform Sub-THz Flux Determination

A simple method for flux scale calibration eliminates the first three sources of errors described above (*i.e.*, errors that are due to atmospheric transmission, temperature scales, and antenna beam aperture efficiencies). In the calibration set of measurements shown in Figure 1 for one 0.2 THz beam, the output data are in ADC units (analog-to-digital conversion). The solar flux to ADC factor can be set directly from the solar disk scans. Solar scans for a single 0.2 THz beam are shown schematically in Figure 2. The solar flux scale for the respective beam is expressed as

$$S = S_{\odot} (\Omega_{\text{beam}} / \Omega_{\odot}) = S_{\odot} (\theta_{\text{beam}} / \theta_{\odot})^2 \text{ SFU}, \tag{1}$$

where S_{\odot} is the full solar disk flux, Ω_{beam} and Ω_{\odot} are the solid angles subtended by the antenna beams and the Sun, respectively, and θ_{beam} and θ_{\odot} are the respective angular sizes ($1 \text{ SFU} = 10^{-22} \text{ Wm}^{-2} \text{ Hz}^{-1}$).

The solar disk flux is reasonably well known, derived from the surface temperature (see, for example, Gezari, Joyce, and Simon, 1973; Shibasaki, Alissandrakis, and Pohjolainen, 2011, and references therein). We have adopted the empirical formula given by Benz (2009) for the range 6–400 GHz:

$$S_{\odot} = 2.79 \times 10^{-5} f^{1.748} \text{ SFU}, \tag{2}$$

where f is the frequency in MHz. We obtain $S_{\odot} \approx 57\,000 \text{ SFU}$ at 0.2 THz and $\approx 176\,800 \text{ SFU}$ at 0.4 THz, respectively.

The ADC-to-flux ratio, k , for each beam is therefore directly derived from the sky-to-Sun observed deflection, Δ_{ADC} , for each of the six beams. The solar flux scale for each beam is set by $S = k \Delta_{\text{ADC}}$, $k = S / \Delta_{\text{ADC}}$, where Δ_{ADC} is the count difference between the solar disk and sky levels of the respective beam. The six SST beam shapes were determined from planet observations (see Kaufmann *et al.*, 2001). They may also be derived from the deconvolution of the solar disk scans. The 0.2 THz HPBW for the four beams are 4 arcminutes. The 0.4 THz beam shapes were more accurately determined, using a beacon transmitter located in the far-field at El Leoncito, being of about 2×3 arcminutes (Kaufmann *et al.*,

2008), which was approximated to 2.5 arcminutes for the application of the method presented here.

It is important to emphasize two advantages of this method to directly calibrate the six beam scales in SFU: a) when the ADC/flux ratio, k , is obtained for each beam, it will remain the same for the flux calculation for bursts located at any position in the solar disk, from center to limb; b) this method determines burst fluxes without the need of corrections for atmospheric transmission and determines the fluxes independently of the antenna temperature of the internal source and from beam gain calibrations. The consistency of this method was verified by comparing the results to flux that was estimated using all corrections for an intense burst observed under good atmospheric transmission and after recent verification of the antenna beam gains and internal temperature scales (Kaufmann *et al.*, 2004).

The SST burst basic identification criteria require that excess time structures are observed in the cluster of the 0.2 THz beams and/or at the 0.4 THz beam at its center. For certain weak events, however, the excess signal is not detectable by all four beams of the cluster. These bursts were identified when observed by at least two of the sub-THz beams (two at 0.2 THz or one at 0.2 THz and another at 0.4 THz). In these cases, the multiple beam technique provides only lower limits of flux estimate, which is good enough for the purpose of this study.

4. Event Analysis

The sub-THz burst search was carried out in time periods for which GOES soft X-ray bursts were reported in the same active region that was tracked by SST. Only well-identified impulsive sub-THz bursts were selected whose the start and peak times were well observed. There were 7751 hours of SST observation under fair to good sky sub-THz transmission conditions, during which 1507 GOES events, of class C or larger, were reported. Of these, 653 occurred in the same active region as tracked by the SST; 564 were class C, 81 class M, and eight class X.

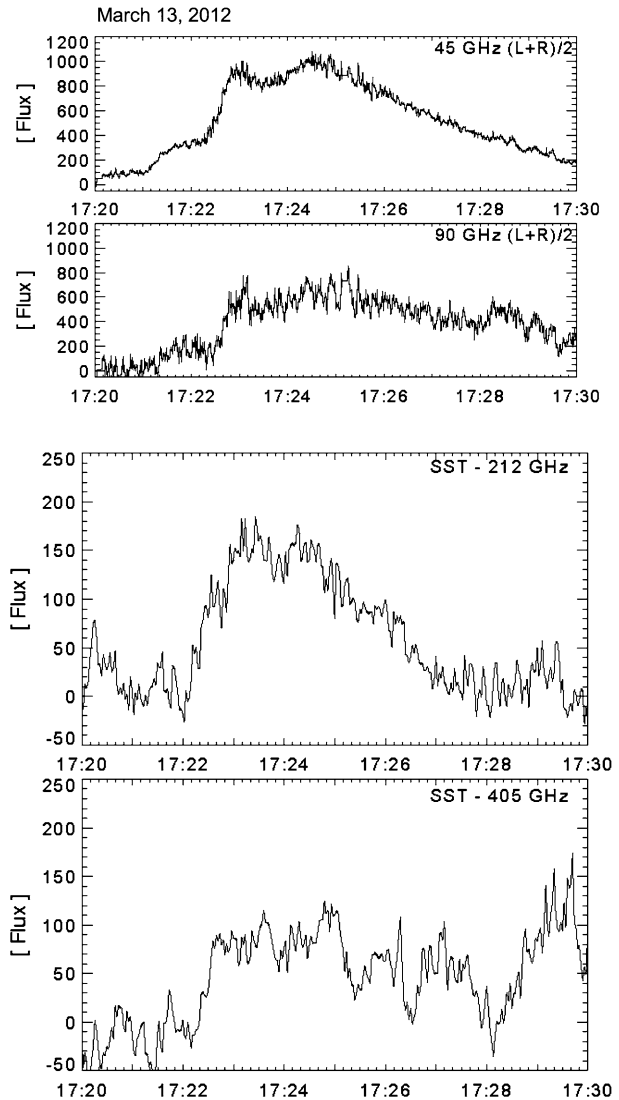
Between 2012 and 2014, 16 sub-THz impulsive bursts were identified: five of them were associated with X-class flares, ten were associated with M-class flares, and one with a C-class flare. This means that 60 % of the X-class flares observed, 12 % of the M-class flares and only 0.2 % of the C-class flares displayed sub-THz emission.

Figures 3, 4, and 5 show examples of three burst time profiles from 45 GHz to 0.4 THz, to illustrate three spectral trends that were found. Their spectra are shown in Figure 6. The peak fluxes shown in Figure 3 (March 13, 2012) decrease with frequency. Figure 4 (February 17, 2013) shows a spectral inflexion that decays at microwaves and increases at sub-THz. Figure 5 (April 12, 2013) displays peaks at sub-THz that do not have a clear counterpart at lower frequencies.

The burst spectra shown in Figure 6 were derived from fluxes at the peak time structures observed at sub-THz and by the RSTN at microwave frequencies 2.69, 4.99, 8.8, and 15.4 GHz, when available. Data obtained by the 45 and 90 GHz patrol telescopes in 2012–2013 were added to the spectra. Table 1 lists the sub-THz events we identified in this study. Approximate r.m.s. errors are indicated. They correspond to the square root of an assumed r.m.s.-equivalent caused by the source position uncertainty squared, added to the signal baseline fluctuation r.m.s. squared. Figure 6 shows the spectra for all events examined here.

We found that seven out of 16 events exhibit spectral maxima in the range 5–40 GHz with fluxes decaying at sub-THz frequencies with about the same spectral indices (three of

Figure 3 The March 13, 2012 sub-terahertz impulsive solar burst time-profile exhibiting fluxes that decrease with frequency, complementing the overall microwave spectrum (see Figure 6 a, second spectrum from the top).

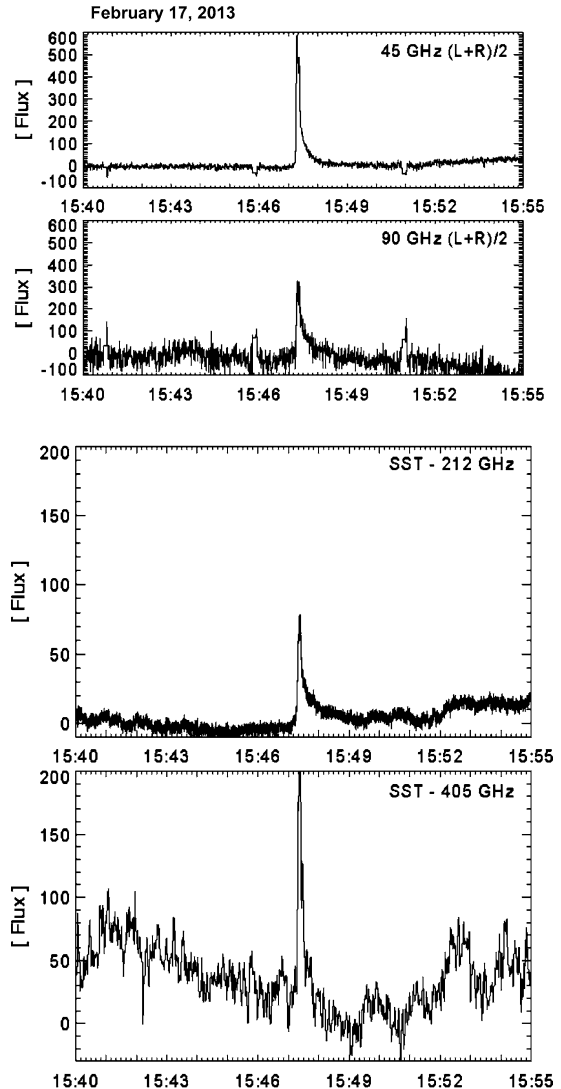


them classified as X, and four as M). Nine out of 16 events exhibited a sub-THz spectral component. Of these, five events exhibited the sub-THz emission fluxes increasing with frequency separated from the microwave spectral component (two classified as X and three as M), and four events have only been detected at sub-THz frequencies (three of them with flux increasing with frequency, associated with M-class GOES events, and one with flux decaying with frequency, associated with the GOES C class event).

5. Discussion and Concluding Remarks

We have analyzed for the first time a collection of sub-THz (0.2 and 0.4 THz) impulsive solar bursts observed by SST, between 2012 and 2014, in the flux range of 10–400 SFU

Figure 4 The February 17, 2013 impulsive solar burst time-profile exhibiting the spectral index sense-reversal feature, negative at microwaves and positive for sub-THz component with fluxes increasing with frequency (see Figure 6 a bottom spectrum).

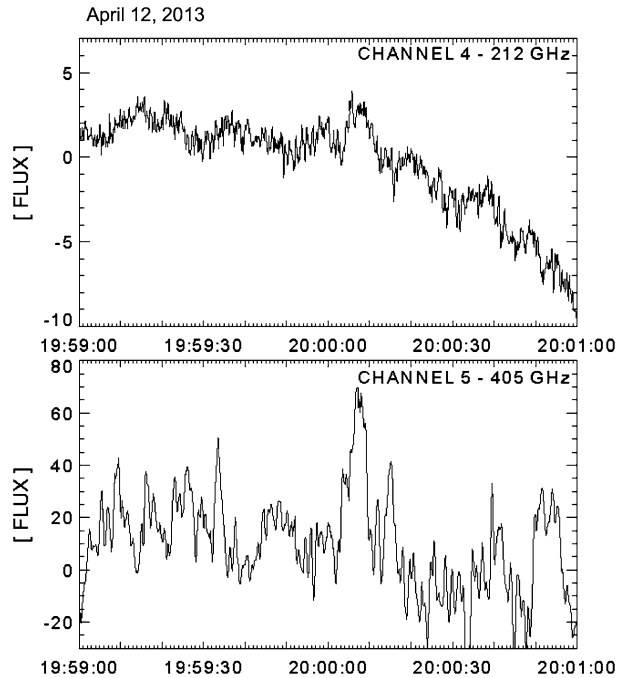


(selected at periods when GOES Class C or larger flares were reported). A simple calibration method has been introduced, setting the flux scale for each SST beam independently of the knowledge of internal temperature scales, antenna beam gains, and atmospheric attenuation. This allowed the selection of a uniform set of 16 bursts for their qualitative comparison.

We found that in the GOES soft X-rays the larger class X generally had a sub-THz impulsive burst associated (five out of eight, or 63 %). The association of sub-THz bursts becomes poor to negligible for smaller GOES class events (ten out of 81 class M, or 12 %, and one out of 564 class C, or 0.2 %).

Analysis of spectral trends has shown that nearly half of the sub-THz bursts (seven out of 16) display flux maxima in the microwave range (5–40 GHz) that decay at 0.2 and 0.4 THz with about the same spectral index. These spectra may be attributed to synchrotron radiation with well-known adopted parameters (Ramaty and Lingerfelter, 1969; Bastian, Benz, and

Figure 5 The April 12, 2013 impulsive solar burst time-profile whose peaks were only observed in the sub-THz range (see Figure 6 b bottom spectrum).



Gary, 1998), whose maximum moves toward higher frequencies for higher electron energies and a stronger magnetic field. The other half of the sub-THz burst set (nine out of 16) exhibits a distinct sub-THz component, in eight of which the flux increases with frequency, and in one the flux decays with frequency. Five bursts exhibit a double spectral structure, one at microwaves, and another at sub-THz. Four bursts exhibited the impulsive time profile at sub-THz, but no peaks at lower frequencies.

Bursts with flux spectra increasing toward THz frequencies, well separated from the well-known microwave spectra, have a similar shape as those obtained in larger bursts (Kaufmann *et al.*, 2004, 2009; Silva *et al.*, 2007). Many models have been suggested to explain them (Kaufmann *et al.*, 2004; Sakai *et al.*, 2006; Silva *et al.*, 2007; Fleishman and Kontar, 2010; Krücker *et al.*, 2013). Two simultaneous spectral components for a single burst, one in the THz range and another in the microwaves, may be conceived of as the composed emission from two distinct sources (Silva *et al.*, 2007). The double spectral feature produced by a single-burst source may also be explained as a result from a microbunching instability on the beams of ultrarelativistic electrons (Kaufmann and Raulin, 2006; Klopff *et al.*, 2014).

The flare THz emission, with fluxes increasing with frequency, might be common to many events if observations were available at higher range of frequencies. Synchrotron radiation peak emission may shift to higher frequencies for electrons accelerated at higher energies, which are not observable by the SST. The sub-THz burst emission spectra might be extended to the 30 THz range where bright impulsive bursts were recently found (Kaufmann *et al.*, 2013, 2015a). However, the 30 THz bursts might also be explained by dense plasma thermal response to the impact of highly energetic particles, radiating at 30 THz and white light (Kaufmann *et al.*, 2015a; Trotter *et al.*, 2015; Penn *et al.*, 2016). These two interpretations require electrons accelerated to very high energies.

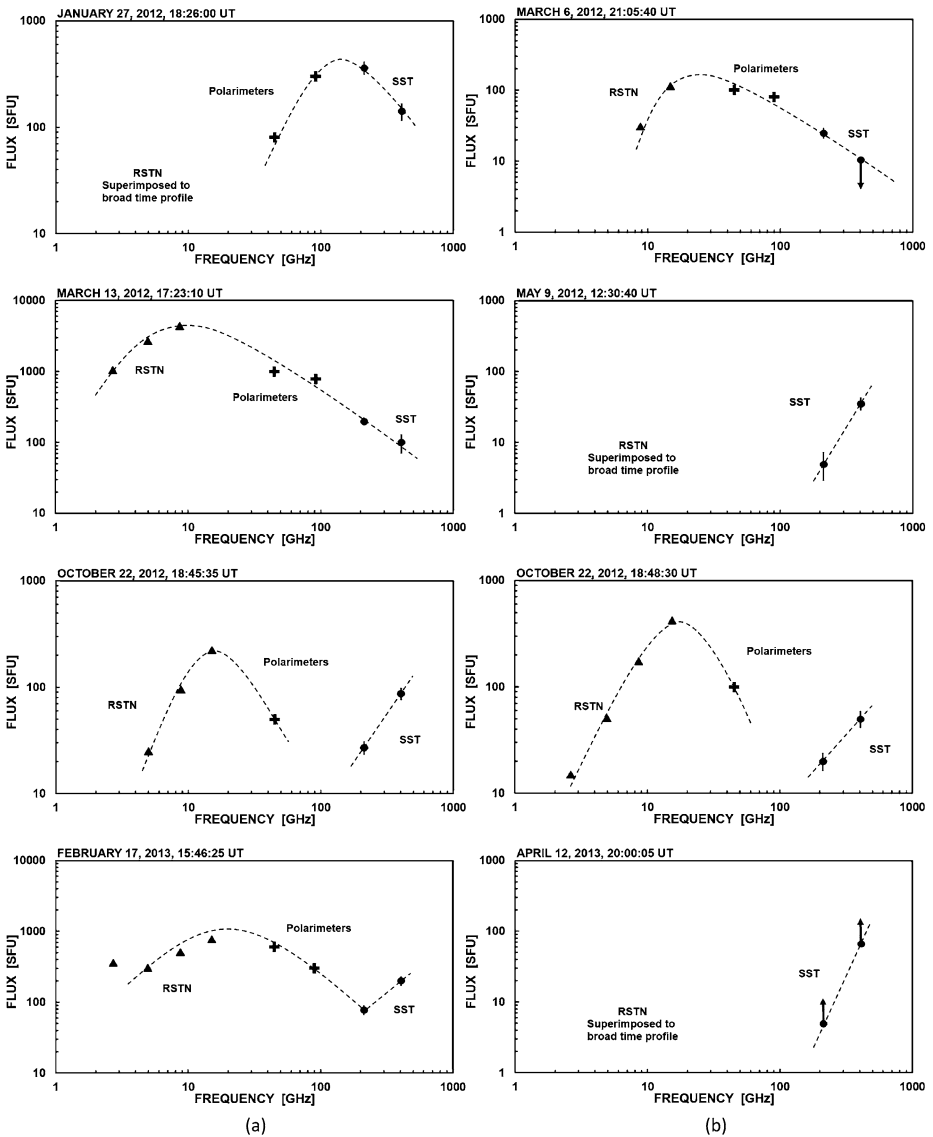


Figure 6 Spectra of all bursts we analyzed in this study. Four bursts were accompanied by an underlying microwave burst component without distinguishable related time structures.

The sub-THz burst identification search in periods of time when there were GOES reported events might not be the most appropriate approach. It has been known that there are a number of significant sub-THz bursts without a clear association with soft X-rays events. This is the case of one burst that is only observed at sub-THz, simultaneously with a fast $H\alpha$ flash, which precedes microwaves and soft X-rays by ten minutes (Kaufmann *et al.*, 2011). Owing to the peculiar unknown characteristics of many sub-THz bursts, we strongly suggest a sub-THz search on all SST data, unbiased by preestablished criteria, to compare the data to events at other energy ranges in a meaningful period of time. This represents a consid-

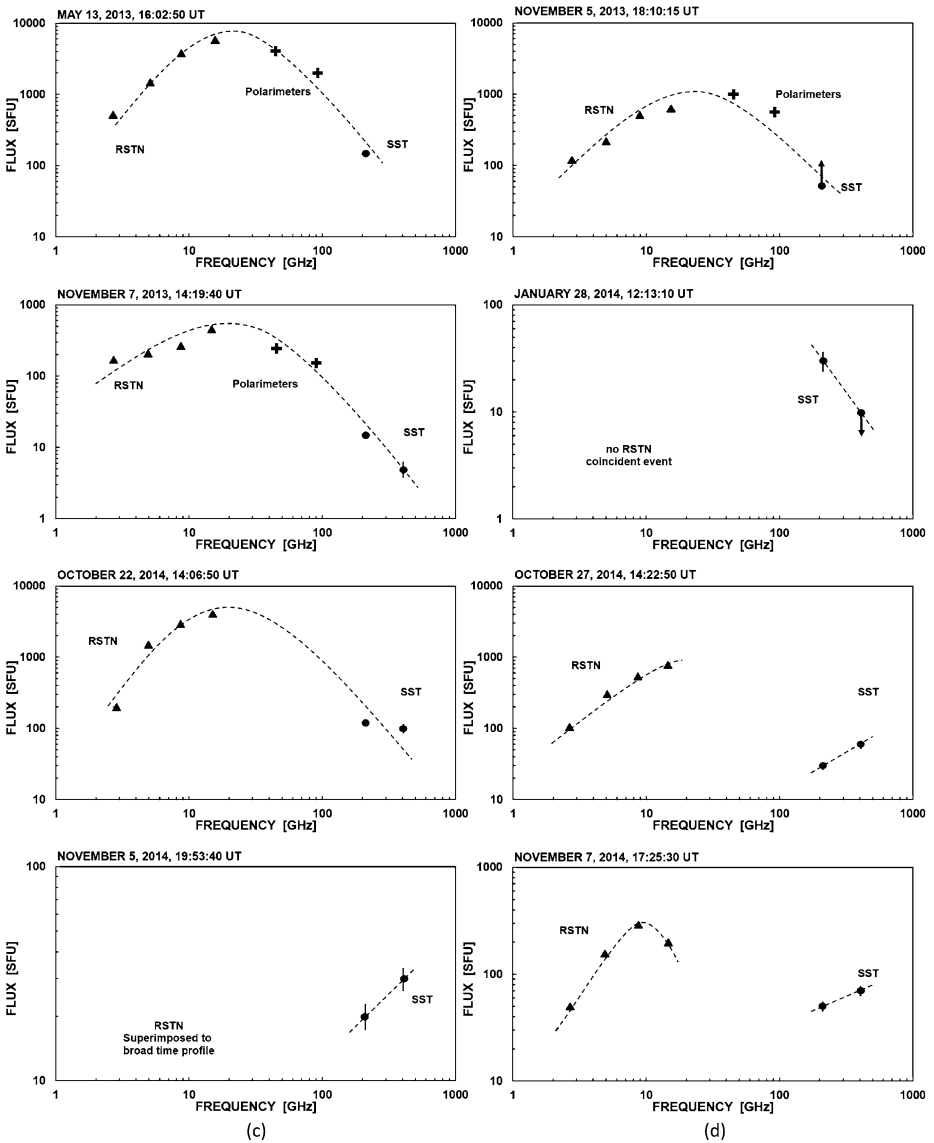


Figure 6 (Continued.)

erable amount of work, which will benefit from the simpler flux scale technique presented here.

Observations at higher THz frequencies are necessary to better understand the spectral trends in the THz range and the respective physical implications. A double photometer experiment at 3 and 7 THz, named SOLAR-T, has recently been flown on a stratospheric balloon mission (Kaufmann *et al.*, 2015b, 2016). The first analyzed burst indicates fluxes that increase with frequency at 0.2 and 0.4 THz as recorded by the SST and at 3 and 7 THz as recorded by SOLAR-T. These time profiles were correlated to bursts at H α and EUV, but

Table 1 The list of sub-THz SST impulsive bursts that were searched for during reported GOES soft X-ray events of class C or larger, for periods common to SST observations, from 2012 to 2014. The last two columns give approximate r.m.s. errors.

List of well identified impulsive sub-THz solar bursts						
Number	Solar burst event	Date	GOES class	SST Peak UT	0.2 THz	0.4 THz
1	SOL2012-01-27T18:26	Jan. 27, 2012	X1.7	18:26:00	360 ± 45	140 ± 23
2	SOL2012-03-06T21:05	Mar. 6, 2012	M1.3	21:05:40	25 ± 4	< 10
3	SOL2012-03-13T17:23	Mar. 13, 2012	M7.9	17:23:10	200 ± 21	100 ± 27
4	SOL2012-05-09T12:30	May 9, 2012	M4.7	12:30:40	5 ± 2	35 ± 6
5	SOL2012-10-22T18:45	Oct. 22, 2012	M5.0	18:45:35	27 ± 4	87 ± 10
6	SOL2012-10-2 2T18:46	Oct. 22, 2012	M5.0	18:48:30	20 ± 3	50 ± 8
7	SOL2013-02-17T15:47	Feb. 17, 2013	M1.9	15:46:25	80 ± 7	200 ± 19
8	SOL2013-04-12T20:00	Apr. 12, 2013	M3.3	20:00:05	5 ± 1	> 70
9	SOL2013-05-13T16:03	May 13, 2013	X2.8	16:02:50	150 ± 14	no data
10	SOL2013-11-05T18:10	Nov. 5, 2013	M1.0	18:10:15	> 50	no data
11	SOL2013-11-07T14:18	Nov. 7, 2013	M2.4	14:19:40	15 ± 2	5 ± 1
12	SOL2014-01-28T12:12	Jan. 28, 2014	C8.3	12:13:10	30 ± 6	< 10
13	SOL2014-10-2 2T14:06	Oct. 22, 2014	X1.6	14:06:50	120 ± 12	100 ± 13
14	SOL2014-10-27T14:21	Oct. 27, 2014	X2.0	14:22:50	30 ± 3	60 ± 6
15	SOL2014-11-05T19:53	Nov. 5, 2014	M2.9	19:53:40	20 ± 3	30 ± 3
16	SOL2014-11-07T17:25	Nov. 7, 2014	X1.6	17:25:30	50 ± 5	70 ± 6

not at X-rays (Kaufmann *et al.*, 2016). A ground-based photometric telescope to operate at higher THz frequency atmospheric windows (0.85, 1.4, and 16 THz) in a high altitude site has recently been completed (Kaufmann *et al.*, 2015b).

Acknowledgements The authors are grateful to the anonymous referee for helpful comments. This research was partially supported by the Brazilian agencies FAPESP (contract No. 2013/24155-3), CNPq, INCT Namitec, Mackpesquisa, US AFOSR, and Argentina CONICET.

Disclosure of Potential Conflicts of Interest The authors declare that they have no conflicts of interest.

References

- Akabane, K., Nakajima, H., Ohki, K., Moriyama, F., Miyaji, T.: 1973, *Solar Phys.* **33**, 431.
- Bastian, T.S., Benz, A.O., Gary, D.E.: 1998, *Annu. Rev. Astron. Astrophys.* **36**, 131.
- Benz, A.O.: 2009, In: Trumper, J.E. (ed.) *Landot-Bornstein – Group IV Astronomy and Astrophysics, Numerical Data and Evolutional Relationships in Science and Technology, Solar System*, **4B**, Springer, Berlin, 103.
- Croom, D.L.: 1971, In: Abrami, A. (ed.) *CESRA-2, Committee of European Solar Radio Astronomers* **2**, 85.
- Fleishman, G.D., Kontar, E.P.: 2010, *Astrophys. J.* **709**, L127.
- Georges, C.B., Schaal, R., Costa, J.R., Kaufmann, P., Magun, A.: 1989, In: *Proc. SBMO Inte. Microwave Symp., São Paulo, 24–27 July 1989, IEEE Cat. No. 89TH0260-0 II*, 447.
- Gezari, D.Y., Joyce, R.R., Simon, M.: 1973, *Astron. Astrophys.* **26**, 409.
- Giménez de Castro, C.G., Raulin, J.-P., Makhmutov, V.S., Kaufmann, P., Costa, J.E.R.: 1999, *Astron. Astrophys.* **140**, 373.
- Guidice, D.A.: 1979 In: *Bulletin of the American Astronomical Society* **11**, 311.
- Kaufmann, P., Correia, E., Costa, J.E.R., Vaz, A.M.Z., Dennis, B.R.: 1985, *Nature* **313**, 380.

- Kaufmann, P., Costa, J.E.R., Gimenez de Castro, C.G., Hadano, Y.R., Kingsley, J.S., Kingsley, R.K., Levato, H., Marun, A., Raulin, J.-P., Rovira, M., Correia, E., Silva, A.V.R.: 2001, In: *Proc. SBMO Int. Microwave Symp., Belem, 6–10 August 2001, IEEE Cat. No. 01TH8568*, 439.
- Kaufmann, P., Raulin, J.-P., Gimenez de Castro, C.G., Levato, H., Gary, D.E., Costa, J.E.R., Marun, A., Pereyra, P., Silva, A.V.R., Correia, E.: 2004, *Astrophys. J.* **603**, L121.
- Kaufmann, P., Raulin, J.P.: 2006, *Phys. Plasmas* **13**, 070701.
- Kaufmann, P., Levato, H., Cassiano, M.M., Correia, E., Costa, J.E.R., Gimenez de Castro, C.G., Godoy, R., Kingsley, R.K., Kingsley, J.S., Kudaka, A.S., Marcon, R., Martin, R., Marun, A., Melo, A.M., Pereyra, P., Raulin, J.-P., Rose, T., Silva Valio, A., Walber, A., Wallace, P., Yakubovich, A., Zakia, M.B.: 2008, *Proc. SPIE* **7012**, 70120L.
- Kaufmann, P., Trottet, G., Giménez de Castro, C.G., Raulin, J.-P., Krücker, S., Shih, A.Y., Levato, H.: 2009, *Solar Phys.* **255**, 31. DOI.
- Kaufmann, P., Marcon, R., Giménez de Castro, C.G., White, S.M., Raulin, J.-P., Correia, E., Olavo Fernandes, L., de Souza, R.V., Godoy, R., Marun, A., Pereyra, P.: 2011, *Astrophys. J.* **742**, 106.
- Kaufmann, P., White, S.M., Freeland, S.L., Marcon, R., Fernandes, L.O.T., Kudaka, A.S., de Souza, R.V., Aballay, J.L., Fernandez, G., Godoy, R., Marun, A., Valio, A., Raulin, J.-P., Giménez de Castro, C.G.: 2013, *Astrophys. J.* **768**, 134.
- Kaufmann, P., Abrantes, A., Bortolucci, E.C., Fernandes, L.O.T., Kropotov, G., Kudaka, A.S., Machado, N., Marcon, R., Nicolaev, V., Timofeevsky, A.: 2015a, In: *26th Intl. Symp. Space THz Technology, Cambridge, MA, 16–18 March 2015*, paper M1-5.
- Kaufmann, P., White, S.M., Marcon, R., Kudaka, A.S., Cabezas, D.P., Cassiano, M.M., Francile, C., Fernandes, L.O.T., Hidalgo Ramirez, R.F., Luoni, M., Marun, A., Pereyra, P., Souza, R.V.: 2015b, *J. Geophys. Res.* **120**, 4155. arXiv.
- Kaufmann, P., Abrantes, A., Bortolucci, E., Caspi, A., Fernandes, L.O.T., Kropotov, G., Kudaka, A., Laurent, G.T., Machado, N., Marcon, R., Marun, A., Nicolaev, V., Hidalgo Ramirez, R.F., Raulin, J.-P., Saint-Hilaire, P., Shih, A., Silva, C., Timofeevsky, A.: 2016, *Am. Astron. Soc., SPD meeting #47*, id. 6.11.
- Klopf, J.M., Kaufmann, P., Raulin, J.-P., Szpigel, S.: 2014, *Astrophys. J.* **791**, 31.
- Krücker, S., Giménez de Castro, C.G., Hudson, H.S., Trottet, G., Bastian, T.S., Hales, A.S., Kasparová, J., Klein, K.-L., Kretzschmar, M., Lüthi, T., Mackinnon, A., White, S.M.: 2013, *Astron. Astrophys. Rev.* **21**, 58. DOI.
- Melo, A.M., Kaufmann, P., Gimenez de Castro, C.G., Raulin, J.-P., Levato, H., Marun, A., Giuliani, J.L., Pereyra, P.: 2005, *IEEE Trans. Antennas Propag.* **53**, 1528.
- Penn, M., Krücker, S., Hudson, H., Murzy, J., Jennings, D., Lunsford, A., Kaufmann, P.: 2016, *Astrophys. J. Lett.* **819**, L30. DOI.
- Ramaty, R., Lingerfelter, R.E.: 1969, *J. Geophys. Res.* **72**, 879.
- Roy, J.-R.: 1979, *Solar Phys.* **64**, 143.
- Sakai, J.I., Nagasugi, Y., Saito, S., Kaufmann, P.: 2006, *Astron. Astrophys.* **457**, 313.
- Shibasaki, K., Alissandrakis, C.E., Pohjolainen, S.: 2011, *Solar Phys.* **273**, 309. DOI.
- Shimabukuro, F.I.: 1970, *Solar Phys.* **15**, 424.
- Silva, A.V.R., Share, G.H., Murphy, R.J., Costa, J.E.R., de Castro, C.G.G., Raulin, J.-P., Kaufmann, P.: 2007, *Solar Phys.* **245**, 311. DOI.
- Tremblin, P., Schneider, N., Minier, V., Durand, G.A., Urban, J.: 2012, *Astron. Astrophys.* **548**, A65.
- Trottet, G., Raulin, J.-P., Mackinnon, A., Gimenez de Castro, G., Simoes, P., Cabeças, D., Luz, V., Luoni, M., Kaufmann, P.: 2015, *Solar Phys.* **290**, 2809. DOI.
- Turner, D.D., Mlawer, E.J., Bianchini, G., Cadetdu, M.P., Crewell, S., Delamere, J.S., Knuteson, R.O., Maschwitz, G., Mlynczak, M., Paine, S., Palchetti, L., Tobin, D.C.: 2012, *Geophys. Res. Lett.* **39**, L10801.
- Valio, A., Kaufmann, P., Giménez de Castro, C.G., Raulin, J.-P., Fernandes, L.O.T., Marun, A.: 2013, *Solar Phys.* **283**, 651.
- White, S.M., Kundu, M.R., Bastian, T.S., Gary, D.E., Hurford, G.J., Kucera, T., Bieging, J.H.: 1992, *Astrophys. J.* **384**, 656.
- Zirin, H., Tanaka, K.: 1973, *Solar Phys.* **32**, 173.